Surface and Interfacial Tension of Cellulose Suspensions

Aline F. Miller* and Athene M. Donald

Polymer and Colloid Group, Cavendish Laboratory, Department of Physics, University of Cambridge, Cambridge, CB3 0HE, United Kingdom

Received April 12, 2002. In Final Form: September 11, 2002

Surface (air−fluid) and interfacial (fluid−fluid) tensions of coexisting isotropic and anisotropic aqueous suspensions of microcrystalline cellulose have been investigated as a function of suspension concentration and ionic strength using the pendant drop method. The surface tension of the individual phases remained constant as concentration was varied within the biphasic region, where the anisotropic surface tension value fluctuated around 72 mN m^{-1} (value for pure water) and the cellulose chains in the isotropic phase displayed surface activity as surface tension was ca. 67 mN m^{-1}. Ionic strength influenced surface characteristics as the surface tension of both phases increases systematically with addition of HCl. Such changes in surface activity are attributed to variations in surface packing density and distribution of the hydrophilic and hydrophobic segments of the cellulose chains. The interfacial tension measurement contrasts such behavior as it remained constant at ca. 10^{-2} mN m^{-1} as a function of both concentration and ionic strength. This value is 3 times that predicted theoretically for an isotropic−anisotropic interface, but this disagreement is thought to reflect the poor estimation of interfacial thickness and the importance of polydispersity in interfacial tension measurement.

Introduction

Surface and interfacial properties play a key role in the phase separation and morphology of phase-separated systems. Model polymer systems have been extensively studied, for example, polymer blends, using a variety of techniques, and all reveal that molecules at the interface differ from those in the bulk with respect to their conformation, intermolecular interaction, and alignment.[1−3] There is increasing evidence that phase separation of macromolecules plays a key role in self-assembly processes in nature.[4−7] In many of these cases, liquid crystallinity of biological macromolecules is of primary importance, for example, in different parts of vertebrates, invertebrates, and plants.[8] The liquid crystalline (LC) structure is present in these examples in the solid state, presumably frozen in as a mesomorph, but what role the fluid LC phase plays in the development of the final structure is still unclear. Furthermore, the LC phase often coexists with a lower concentration isotropic phase, and during self-assembly processes the interface between the two phases is likely to have a crucial role as it divides the regions which have self-assembled from those which have not, as the self-assembly front advances. The nature of this interface, and its corresponding interfacial tension, will determine to a large extent the overall fluidity of such systems: the higher the interfacial tension, the more resistant the whole system will be to deformation and flow. We have attempted, therefore, to identify the fundamental phenomena that govern an isotropic−anisotropic interface, such as intermolecular interaction and alignment of molecules at the fluid surface and interface by investigating the surface and interfacial tension values of one system. The system chosen was microcrystalline suspensions derived from cellulose, as these have recently been shown to undergo a phase separation into isotropic and cholesteric phases within a narrow concentration range.[9−11] Moreover, properties such as rod length, concentration, and electrostatic charge can easily be varied to explore a wide range of parameter space.

The phase behavior of the cellulose suspensions has been extensively studied by Gray and co-workers;[12,13] hence in this paper we will only summarize the characterization and phase transitions of the cellulose suspensions we prepared, before concentrating on surface and interfacial measurements. The surface tension (air−fluid) of both isotropic and anisotropic phases is discussed as a function of suspension concentration and ionic strength. Thereafter, interfacial tension measurements as a function of concentration will be discussed and compared with recent experiments by Chen and Gray.[14] The suspensions they studied contained cellulose chains of comparable length to those analyzed here but were prepared using different treatment conditions. This possibly led to the introduction of different quantities and densities of charged sulfate ester groups in comparison to our system. Moreover, the results they presented were over a limited concentration range, at one ionic strength, and were determined using an alternative method. Here we examine fully the influence of both concentration and ionic strength,

* Corresponding author. New address: Department of Chemical Engineering, UMIST, P.O. Box 88, Manchester, M60 1QD, U.K. E-mail: aline.miller@umist.ac.uk.

(1) Jones, R. A. L.; Richards, R. W. *Polymers at Surfaces and Interfaces*; Cambridge University Press: Cambridge, 1999.
(2) Xing, P. X.; Bousmina, M.; Rodrigue, D.; Kamul, M. R. *Macromolecules* **2000**, *33*, 8020.
(3) Ajji, A.; Utracki, L. A. *Polym. Eng. Sci.* **1996**, *36*, 1574.
(4) Rill, R. L.; Livolant, F.; Aldrich, H. C.; Davidson, M. W. *Chromosoma* **1989**, *98*, 280.
(5) Suzuki, A.; Maeda, T.; Ito, T. *Biophys. J.* **1991**, *59*, 25.
(6) Viney, C.; Hober, A. E.; Verdugo, P. *Macromolecules* **1993**, *26*, 852.
(7) Viney, C.; Kerkam, K.; Gilliland, L.; Kaplan, D.; Fossey, S. *MRS Proc.* **1992**, *248*, 89.
(8) Neville, A. C. *Biology of Fibrous Composites*: *development beyond he cell membrane*; Cambridge University Press: Cambridge, 1993.
(9) Revol, J. F.; Bradford, H.; Giasson, J.; Marchessault, R. H.; Gray, D. G. *Int. J. Biol. Macromol.* **1992**, *14*, 170.
(10) Revol, J. F.; Godbout, L.; Dong, X. M.; Gray, D. G. *Liq. Cryst.* **1994**, *16*, 127.
(11) Revol, J. F.; Godbout, L.; Gray, D. G. *J. Pulp Pap. Sci.* **1998**, *24* (5), 146.
(12) Dong, X. M.; Kimura, T.; Revol, J. F.; Gray, D. G. *Langmuir* **1996**, *12*, 2076.
(13) Fleming, K.; Gray, D. G.; Matthews, S. *Chem.—Eur. J.* **2001**, *7*, 1831.
(14) Chen, W.; Gray, D. G. *Langmuir* **2002**, *18*, 633.

10.1021/la0258300 CCC: $22.00
Published on Web 11/22/2002

before finally comparing results with theoretical predictions for the interfacial behavior of rigid rod polymers.

Experimental Section

Sample Preparation. The cellulose suspensions were prepared by acid hydrolysis as outlined in detail in refs 9−11. The resulting hydrolyzed, charged suspensions were maintained at a constant ionic strength by extensive dialysis against 0.01 M HCl, before reducing the polydispersity of the axial ratio by size fractionation. This was achieved by concentrating the suspension via evaporation until 20% of the solution was anisotropic. This anisotropic lower phase was discarded, and the remaining suspension was concentrated further until only ca. 20% remained isotropic. The upper phase was also discarded and the process repeated to ensure the removal of extra long and short length rods. Concentrated stock samples were subsequently obtained by evaporation and stored in the refrigerator until required. A series of concentrations were prepared by careful dilution with distilled water, and the desired concentration of HCl was added until all solutions were at a constant pH.

To investigate the effect of ionic strength, stock suspensions of concentrated cellulose were prepared and aliquots diluted with different concentrations of acid until the total concentration of cellulose was constant, and the pH was determined.

Isotropic/anisotropic volume fractions were measured by placing each homogeneous suspension in a sealed glass vial (5 cm high with a 2 cm diameter), exposing the solution for 1 min in the ultrasonicator, and allowing 2−3 days for equilibration. Any phase separation was quantified simply by measuring the height fraction of each phase using a ruler.

Microcrystalline Characterization. *Density Measurements.* The suspension density, ρ, was determined using a PAAR digital density meter (Paar Scientific Ltd.) over a wide concentration range encompassing both the isotropic and anisotropic phases. Each phase was placed in a 1 cm^3 U-shaped tube, and the temperature was regulated at 296 ± 0.5 K. The data for the suspension diluted only by water fall on a straight line with gradient 0.005 g cm^{-1}. This graph facilitated the estimation of the weight concentration of cellulose in an unknown sample from its density.

Polarizing Microscopy. The texture of the liquid crystalline phase was determined by pipetting an aliquot from each sample into a flat glass tube, 0.4 mm wide, sealing the tube at both ends and viewing it through crossed polars (Zeiss universal microscope). The chiral nematic pitch was determined by measuring the distances between the fingerprints using a calibrated slide.

Transmission Electron Microscopy. Dimensions of the rods were measured using a transmission electron microscope (TEM, Joel 200EX). Samples were prepared by drying a drop of sample (0.5%) onto a carbon-coated microscope grid (Agar) and staining using a 0.5% aqueous solution of uranyl acetate (Sigma).

Surface Tension Measurements at the Air−Liquid Interface. The surface activity of the isotropic and anisotropic phases was determined by the pendant drop method using a dynamic contact angle instrument (FTÅ 200 instrument from Camtel Ltd.). The coexisting phases were macroscopically separated by syringing off the upper isotropic phase. Each phase was subsequently sucked independently into a microsyringe with a flat leur tip and placed into the instrument where the syringe tip resided in an empty cuvette cell with a Teflon cap to minimize evaporation and sample contamination. A controlled volume of suspension was pumped into the empty cell (typically 20 μL at a speed of 1 μL s^{-1}) to form a pendant drop. Measurements reported here were taken at 296 ± 0.5 K. Drop formation and equilibration were recorded by collecting a series of images over time intervals ranging from 0.5 to 60 s (user defined) for up to 4 h. The characteristic density value for each phase was entered into the instrument software, and the surface tension values were determined by drop shape analysis based on the Bashforth−Adams technique for solving the Laplace−Young equation.[15] Careful calibration of the instrument was performed using doubly distilled water.

(15) Bashforth, F.; Adams, J. C. *An Attempt to Test the Theories of Capillary Action*; Cambridge University Press: Cambridge, 1883.

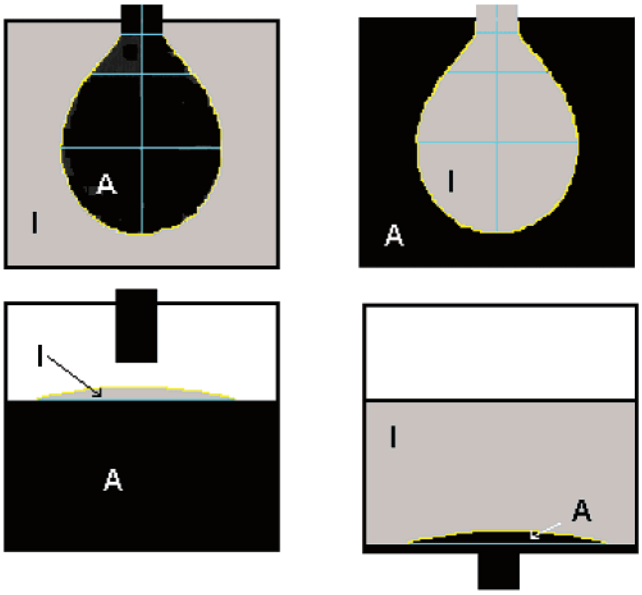

Figure 1. Schematic representation of the different methods attempted to measure the isotropic−anisotropic interfacial tension: (a) suspend a pendant drop of anisotropic phase in isotropic media, (b) suspend an isotropic drop in anisotropic media, (c) introduce a sessile drop of isotropic phase on top of anisotropic phase, and (d) introduce a sessile drop of anisotropic phase onto the base of the sample cell while surrounded by isotropic media.

Interfacial Tension Measurements. Interfacial tension measurements were more difficult, and various strategies were employed (for a summary see Figure 1). Attempts included introducing a pendant drop of anisotropic phase into an isotropic media (Figure 1a), introducing an isotropic drop into an anisotropic phase (Figure 1b), introducing an isotropic sessile drop on top of an anisotropic phase (Figure 1c), and finally introducing the anisotropic phase into an isotropic media as a sessile drop (Figure 1d). The bulk media was always contained within a square cuvette cell of 10 mm diameter, and the drop-forming phase was introduced via a microsyringe.

Sample leakage, solvent evaporation, and contamination were minimized by placing a glass (or Teflon) lid, with a small hole for the syringe tip, onto the base of the sample. The first three sets of experiments were all unsuccessful (Figures 1a−c) as no drop could be formed, stable or otherwise. The density of each phase was also varied (to match and also contrast) in an attempt to facilitate drop formation, but this also proved unsuccessful. In the first experiment, no pendant drop formed as the dense liquid crystalline phase immediately formed a stream and sunk to the bottom of the sample cell. The anisotropic phase proved too dense to allow imaging of isotropic drop formation, and the isotropic sessile drop on anisotropic substrate spread within milliseconds to completely wet the surface. The last set of experiments (Figure 1d) were successful, however, but were dependent on the composition of the substrate. Typically, a controlled volume (∼10 μL) of anisotropic phase was pumped into the isotropic media to form the sessile drop (formed in preference to an inverted pendant drop since the anisotropic drop was the denser of the two phases). When Teflon was used as the base, the sessile drop completely displaced the isotropic media and wet the hydrophobic surface within seconds; hence no equilibrium interfacial tension was accessible. This wetting phenomenon is due to the anisotropic phase being hydrophobic in comparison to the isotropic phase ($\gamma_{aniso} > \gamma_{iso}$); hence the anisotropic phase preferentially wets the Teflon surface minimizing surface energy. The other substrate used was glass, which is hydrophilic in comparison. In this case, the anisotropic drop formed was more stable due to the isotropic phase preferentially wetting the glass surface.

The alternative route, adopted by Chen and Gray,[14] to sessile drop formation involved dispersing an anisotropic drop from above, allowing it to sink to the bottom of the sample cell and

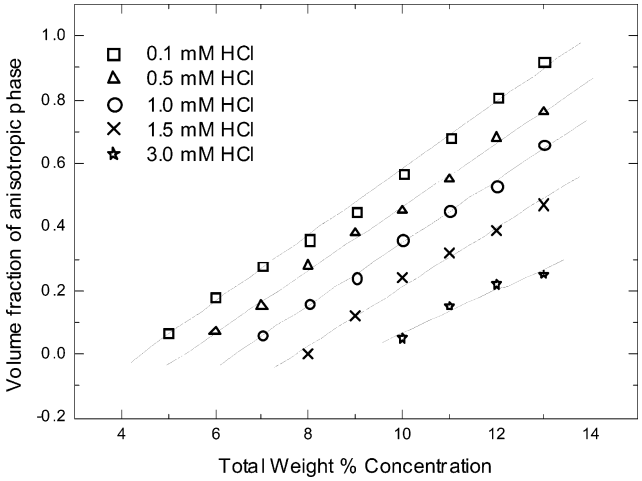

Figure 2. Phase diagram of an aqueous microcrystalline suspension of cellulose as a function of concentration for a range of ionic strengths.

equilibrate before predicting the radius of curvature and shape factor of the sessile drop using a least-squares fitting method[16] based on the Young−Laplace equation. Chen and Gray subsequently calculated surface tension from the shape factor. We also employed this method of drop formation for comparative purposes.

In both experimental scenarios, images of drop formation and equilibration were collected at 0.5 s intervals for $^3/_4$ h at which point constant values were obtained. Each image was subsequently analyzed using computer software, again using the Bashforth−Adams technique,[15] and no difference between methods (introduction of sessile drops from below and above) was observed. The pendant drop analyzer was placed on an antivibration table as slight agitation disrupted equilibrium and led to the sessile drop simply wetting the glass surface.

Results and Discussion

Phase Behavior. Figure 2 shows the phase behavior where the total suspension concentration ranged between 1 and 14 weight percent (wt %). Above a lower critical concentration (5 wt %, for 0.1 mM HCl for example), a biphasic suspension formed with a sharp phase boundary. The lower of the two phases displayed liquid crystalline characteristics under the polarizing microscope where nematic "tactoids"[9] were initially viewed, but these equilibrated over time (a few hours to 2 days) to produce textures indicative of a chiral nematic (cholesteric) liquid crystalline phase. The upper, less dense phase was isotropic. Such biphasic behavior was only present in a narrow concentration window as the isotropic phase only occurred below a critical concentration (14% for the 0.1 mM HCl sample). The critical concentrations for the onset and upper limit of biphasic behavior will be referred to as c^* and c^{**}, respectively, in accordance with standard usage. All results are in agreement with the studies of Dong and co-workers[12] where the volume fraction of anisotropic phase increased linearly with concentration but decreased linearly with increasing added electrolyte. Furthermore, an increase in magnitude of both c^* and c^{**} was observed with increasing ionic strength.

Phase separation and interfacial tension are predicted to be highly dependent on the concentration of the individual coexisting phases;[17−20] therefore individual

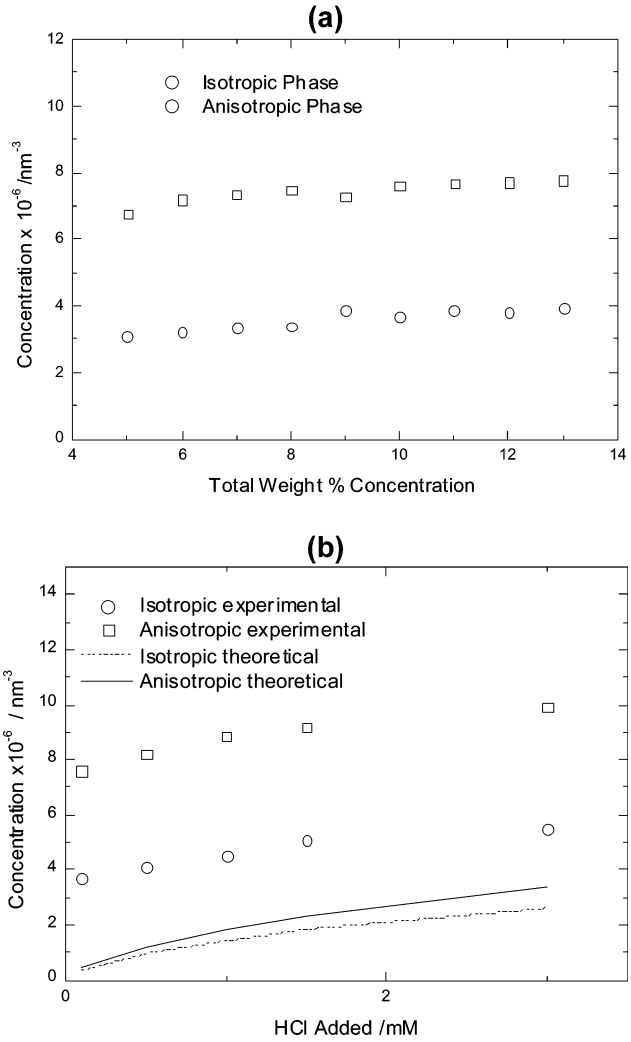

Figure 3. Individual concentrations of isotropic and anisotropic phases as (a) a function of total suspension concentration for samples with a constant pH of 4.0 and (b) a function of ionic strength with a constant concentration of 10 wt % (6.34×10^{-6} nm^{-3}) (the solid and dashed lines show anisotropic and isotropic theoretical predictions, respectively).

wt % concentrations were determined for each of the cellulose phases. The wt % results were converted into number density concentrations, c, using $c = w/\{[w + (100 - w)\rho]LD^2\}$ where w is the wt % concentration (anisotropic, wt $\%_{aniso}$; isotropic, wt $\%_{iso}$), ρ is the density of cellulose (1.6 g cm^{-3} from Aldrich), and L and D are the hard-core rod length and diameter, respectively. This calculation enables direct comparison with theoretical predictions. The number density concentrations for both isotropic and anisotropic phases were determined (see Figure 3a for data where the total suspension pH was fixed at 4.0 (0.1 mM HCl)), but no significant trend is observed with total suspension concentration (gradients of the data collected are close to zero), indicating the concentrations of the coexisting phases are insensitive to suspension concentration at constant ionic strength. This is expected since the effect of electrostatic interaction on phase separation will remain constant as suspension concentration is increased[21] and is in agreement with theoretical predictions (constant values of 6.59×10^{-6} and 8.44×10^{-6} nm^{-3} calculated for the isotropic and anisotropic phases, respectively). The effective rod diam-

(16) Rotenberg, Y.; Boruvka, L.; Neumann, A. W. *J. Colloid Interface Sci.* **1983**, *93*, 169.
(17) Stroobants, A.; Lekkerkerker, H. N. W.; Odijk, T. *Macromolecules* **1986**, *19*, 2232.
(18) Sato, T.; Teramoto, A. *Physica A* **1991**, *176*, 72.
(19) Lee, S. D. *J. Chem. Phys.* **1987**, *87*, 4972.
(20) Odijk, T. *Macromolecules* **1986**, *19*, 2313.
(21) Manning, G. *J. Chem. Phys.* **1969**, *51*, 924.

Table 1. pH and Surface and Interfacial Tension Data for Aqueous Suspensions of Microcrystalline Cellulose at pH 4.0 within the Biphasic Region

	wt % concentration						
	2	4	6	8	10	12	14
pH_{iso}	4.08	4.05	4.10	4.12	4.06	4.08	4.11
pH_{aniso}	3.96	3.95	3.92	3.93	3.88	3.95	3.96
$\gamma_{iso\ expt}$/mN m^{-1}	66.3	66.2	65.8	66.3	66.5		
$\gamma_{aniso\ exp.}$/mN m^{-1}			70.9	70.7	71.3	72.9	73.4
$\gamma_{aniso-iso\ expt}$/ mN m^{-1}			0.014	0.013	0.010	0.012	

eter, and hence c_{iso} and c_{aniso}, will therefore also remain constant leaving only the volume fraction of each phase to vary with suspension concentration. Experimentally, the concentration of the anisotropic phase (c_{aniso}) was always ca. 4×10^{-6} nm^{-3} higher than the corresponding isotropic concentration (c_{iso}). This difference between the coexisting phases leads to a small disparity in the pH (typical results are given in Table 1) where the pH of each phase was constant throughout the suspension concentration range, but the anisotropic values were always slightly lower than their isotropic counterpart. The difference between the different phases is attributed to partitioning of the rods, where the longer, heavier rods carrying more charged sulfate ester groups will settle preferentially in the lower, anisotropic phase.

The individual phase concentrations were also determined as a function of ionic strength and are given in Figure 3b for a constant concentration of 10 wt %. It is evident that phase concentration increases with increasing ionic strength, which agrees qualitatively with theory (lines in Figure 3b). The concentrations are, however, consistently underestimated. This quantitative discrepancy between experiment and theory is thought to be due to the polydispersity of the cellulose rods and coagulated flocs that may be present in the suspension. Theory does not account for such factors, yet a wide distribution was observed in the TEM micrographs ($L = 180 \pm 30$ nm and $D = 8 \pm 3$ nm), despite size fractionation experiments. Furthermore, one of the theoretical conditions has not been met experimentally, as we are not working in excess salt conditions. Details of calculations and a complete comparison between experiment and theory can be found in Dong et al.[12]

Surface Tension Measurement. Air−liquid surface tensions were determined by suspending a drop of liquid phase into an enclosed cuvette cell and analyzing its shape over time. Equilibration of each pendant drop was monitored immediately after drop formation by collecting images at 0.5 s intervals for 5 min; then intervals were extended to 30 s for a total of 4 h. Results for one such experiment are given in Figure 4a where the drop formed was from the isotropic phase of a 5 wt % concentration. A rapid decrease in magnitude (ca. 1.5 mN m^{-1}) was observed over the first 30 s. Thereafter, the surface tension remained constant at a value of 66.2 ± 0.5 mN m^{-1}. Such changes were also observed qualitatively as the drop shape became more elongated before reaching a constant, equilibrated conformation as time elapsed. The average time for equilibration increased as the suspension became more concentrated, presumably due to the accompanying increase in viscosity reducing the mobility of the cellulose chains at the air−water interface. All surface tensions quoted here are therefore equilibrium values taken 20 min after drop formation.

This experimental procedure was repeated three times, and results were averaged for all phases, concentrations, and ionic strengths. Surface tension values for each phase

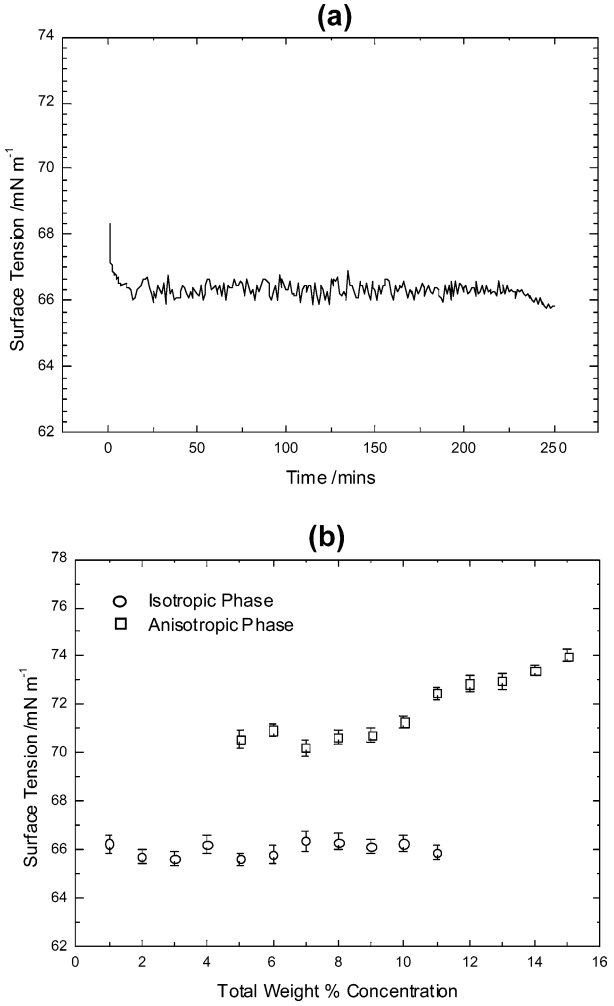

Figure 4. Variation of surface tension of (a) an isotropic drop over time (phase formed from a suspension of total concentration 5 wt % with pH 4.0, 0.1 mM acid) and (b) isotropic and anisotropic phases as a function of total suspension concentration at constant ionic strength (pH 4.0, 0.1 mM acid).

with a constant total suspension pH of 4.0 (0.1 mM acid) are given in Table 1 and compared in Figure 4b. It is evident that the surface tensions of both the isotropic (γ_{iso}) and anisotropic (γ_{aniso}) phases are approximately constant over the biphasic concentration range. The isotropic values differ significantly, however, from their anisotropic counterparts where the former is ca. 66.2 ± 0.5 mN m^{-1}, which is systematically ∼5 mN m^{-1} lower than γ_{aniso}. The magnitude of γ_{aniso} is centered around the surface tension of pure water (72 mN m^{-1}), indicating the cellulose rods are not surface active in the liquid crystalline phase. A slight increase in this value is observed above c^{**}, signifying the number of thermodynamically favorable interactions at the near surface is reduced at high concentrations (i.e., $\gamma_{aniso} \geq 72$ mN m^{-1}) due to a variation in the hydrophobic/hydrophilic balance. To identify what mechanism is causing such change and to explain the difference between γ_{iso} and γ_{aniso}, we first need to identify the factors that influence surface tension.

Surface effects can be expressed in terms of Gibbs energy where the work, W, required to change the surface area, A, by an infinitesimal amount dA is $dW = \gamma\, dA$, where the constant of proportionality, γ, is the surface tension. Surface activity is a balance between hydrophilic and hydrophobic components and is a measure of how well the two can separate at the air−liquid interface. The greater the separation of the hydrophilic/hydrophobic

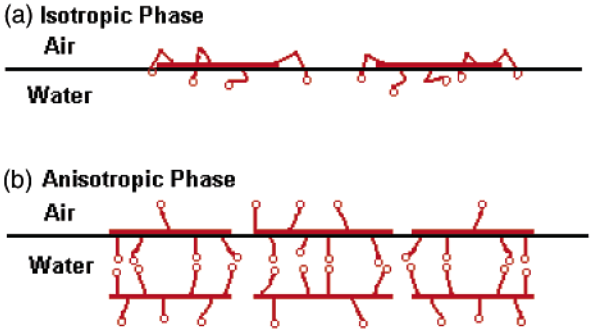

Figure 5. Schematic of the organization of cellulose chains positioned at the air−water interface in the (a) isotropic and (b) anisotropic phases. The cellulose backbones are represented by the red lines, and the charged sulfate ester groups by circles.

segments, the less work required for increasing surface area, and hence the lower the surface tension. Cellulose chains are rigid and contain both polar (ether, hydroxyl, and ester) and nonpolar (CH and CH_2) groups distributed along the length of the chain; therefore any change in γ must be due to a change in the surface forces as the cellulose chains reorganize. It is clear from the surface tension studies presented here, that is, $\gamma_{iso} < \gamma_{aniso} \geq 72$ mN m^{-1}, that the hydrophobic/hydrophilic groups are at least partly separated at the near surface in the isotropic phase where the polar and nonpolar groups are assumed to reside in the water and air phases, respectively, leading to a reduction in γ_{iso} from pure water. In the anisotropic phase, the molecules must be in a conformation where the two groups are no longer able to be well separated, because $\gamma_{aniso} > \gamma_{iso}$. Furthermore, the increase in γ_{aniso} as the concentration surpasses c^{**} (ca. total wt % = 12) suggests a further disruption to the hydrophobic/hydrophilic distribution.

The surface conformation of the cellulose rods has been studied, using optical and environmental scanning electron microscopy (ESEM), and the rods are known to lie in the surface plane in both the isotropic and anisotropic phases.[12,22] However, in the isotropic regime the chains are randomly distributed in the isotropic phase, whereas they are highly oriented in the anisotropic media. Such different molecular packing will result in different intermolecular interactions and hydrophilic/hydrophobic segment distributions. Presumably there is little intermolecular interaction in the isotropic phase as the rods are well separated (surface area per chain is high), thus providing sufficient space and freedom for each glucose monomer to rotate and bend around the ether linkage to maximize favorable molecule−subphase interactions (assuming the system adopts the conformation of lowest energy). The driving force for liquid crystalline behavior is the intermolecular hydrogen bonding that occurs along the length of the rods as they align parallel with each other. Such bonding involves the hydrophilic side groups, and to maximize interaction the ether linkages and six-member glucose rings will twist and align with respect to each other. These differences in molecular orientation between isotropic and anisotropic phases are schematically outlined in Figure 5, parts a (isotropic) and b (anisotropic). The hydrogen bonding which forms at the onset of anisotropy will increase the energy cost of any reorientation of the hydrophilic groups toward the surface. Consequently, surface tension is high in comparison to the isotropic media. No variation in either value was noted, however, as the suspension concentration increased within

(22) Miller, A. F.; Donald, A. M. Unpublished results.

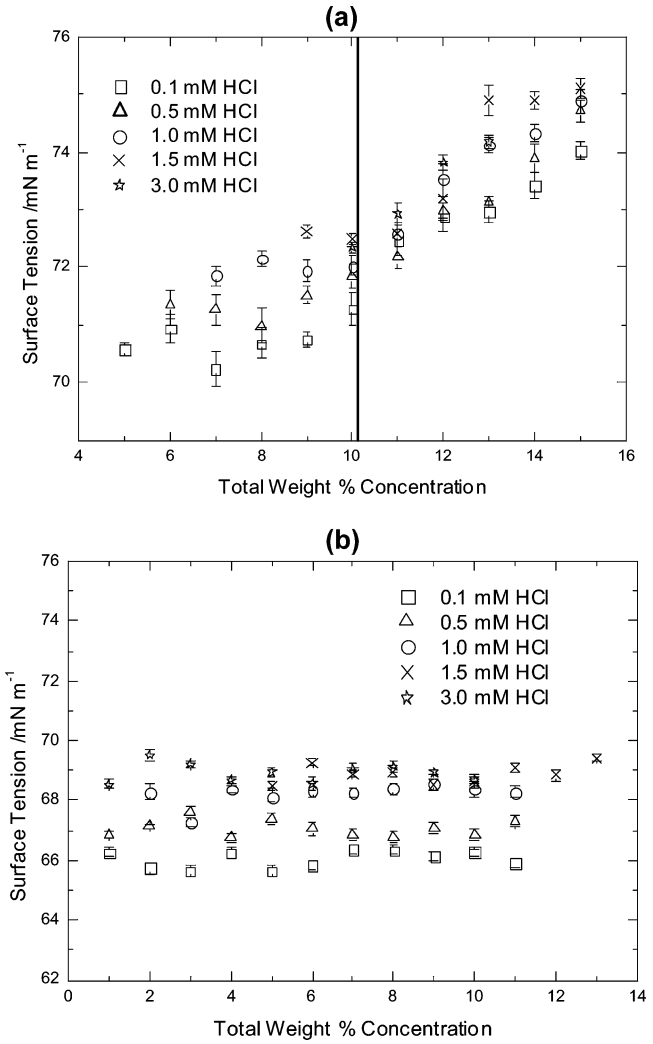

Figure 6. Variation in surface tension of (a) anisotropic and (b) isotropic phases as a function of total suspension concentration for a range of ionic strengths.

the biphasic region, due to the constant concentration of the individual isotropic/anisotropic phases.

As the concentration of the liquid crystalline phase increases above c^{**}, the intermolecular distance reduces due to increased packing density of the rods and accompanying increasing strength of the intermolecular hydrogen bonding. Such changes in surface organization will further reduce any reorientation ability of the glucose monomers. Hence the number of favorable hydrophilic/water interactions will decrease. This effect will become more dominant with increasing concentration and is reflected in the continual rise in γ_{aniso}. Supporting evidence for this hypothesis comes from analysis of the cholesteric pitch of the anisotropic phase. The pitch is a measure of cellulose interactions (smaller pitch, stronger interaction) and is observed, both theoretically and experimentally, to decrease monotonically with increasing concentration.[12,21,22] This decreasing intermolecular distance will reduce chain flexibility and hence the ability for monomer segments to reorientate and maximize favorable hydrophilic/water interactions at the near surface. An increase in surface tension is therefore observed.

Results for the influence of suspension ionic strength on surface tension, summarized in Figure 6, reveal that behavior can again be split into two regimes: one above and one below c^{**}. Within the biphasic regime, γ_{iso} and γ_{aniso} remain constant for all ionic strengths, and above

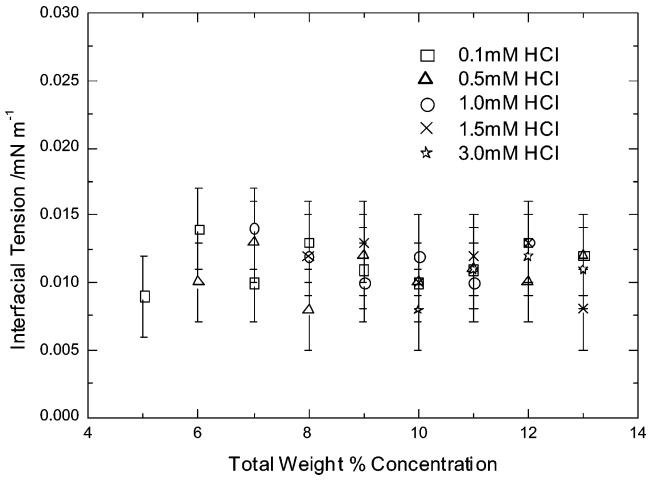

Figure 7. Interfacial surface tension as a function of total suspension concentration and ionic strength.

$c^{**}\,\gamma_{aniso}$ increased linearly with identical dependencies for each sample. Moreover, all isotropic and anisotropic phases display a dependence on ionic strength where the surface tension of each phase increases with increasing ionic strength. Differences between the surface tensions for each ionic strength are small but are nonetheless real as they are highly reproducible within experimental error. All values given here were recorded at a constant temperature of 296 ± 0.5 K as small differences in temperature led to a significant variation in surface tension values: a variation of 3 K for example altered the surface tension by ca. 0.5 mN m^{-1}. The influence of ionic strength is again attributed to changes in surface density and orientation of the cellulose chains. It was noted earlier (Figure 3b) that the concentrations of the isotropic and anisotropic phases increase with increasing ionic strength. Increasing ionic strength must therefore be reducing the screening effect, as expected, of the charges along the rod allowing the chains to move closer together. Addition of acid to the suspension is known to reduce the chiral nematic twist of the liquid crystalline media;[12,22] therefore the packing density on the surface increases, inhibiting molecular ability to separate hydrophilic and hydrophobic segments, giving rise to the increase in γ_{aniso}.

Interfacial Tension Measurement. Careful drop shape analysis of all images using computer software permitted the contact angle and subsequently isotropic−anisotropic interfacial tension ($\gamma_{aniso-iso}$) to be determined. Both experimental methods (the method outlined schematically in Figure 1d and that used by Chen and Gray;[14] for further details see Experimental Section) gave comparable results within the limit of error, where the magnitude of inaccuracy was ca. 10% due to the roughness of the interface and not the drop preparation or analysis method. Each data point is therefore an average of eight experiments; four for each method of drop formation. Results showing the influence of concentration on interfacial tension for each ionic strength are summarized in Figure 7, and a selection is presented in Tables 1 and 4. The results reveal that both concentration and ionic strength play a minimal role in interfacial tension, as all values are consistently low at ca. 0.011 ± 0.003 mN m^{-1}. It is known that interfacial tension is closely related to the concentration difference between the coexisting phases; for example, if the concentration between phases became closer (i.e., wt $\%_{aniso}$ − wt $\%_{iso}$ decreases) then the concentration gradient across the interface would decrease and this would be reflected in a reduction of interfacial tension. Since the total suspension concentration did not affect the concentration difference of individual phases (see Figure 3), no change in $\gamma_{aniso-iso}$ was anticipated with either suspension concentration or ionic strength.

The values observed here are however approximately 2 orders of magnitude higher than those obtained by Chen and Gray.[14] Our experimental procedures are comparable; therefore the nature of the sample and its environment must be responsible for this discrepancy. One possibility is the variation in density of the charged groups along each chain introduced by the different acid hydrolysis conditions. We have shown that if suspensions are prepared using the same batch of cellulose and identical treatment processes then the surface charges introduced are comparable (determined by conductometric titrations[23]). Chen and Gray[14] used a different batch of cellulose and moreover alternative preparative conditions were used (temperature, hydrolysis time), which could contribute to the different interfacial tension results. This possibility remains ambiguous, as unfortunately it is difficult to locate surface charge on individual rods. It is also possible that the differing batches of cellulose could contain different surface-active impurities that could influence the results.

Comparison with Theory. Experimental results show that phase behavior and surface tension of the cellulose suspensions are dependent on concentration and ionic strength whereas interfacial tension displays no such relationship. The phase behavior of our system is in good agreement with that extensively discussed by Dong and co-workers;[12] therefore we will concentrate on the surface and interfacial properties.

Several authors have theoretically calculated the properties of the isotropic−anisotropic interface, such as density profile, molecular orientation, and interfacial tension. The majority of the theoretical work has been based on Onsager's free energy density expression[24] using the second virial approximation, where the phase behavior for solutions of monodisperse, hard, rigid rodlike molecules has been predicted. Differences between the numerous theories have evolved from difficulties in solving the interfacial properties analytically, as these have forced assumptions to be made regarding the concentration and degree of molecular orientation at the interface. Initially Doi and Kuzuu[25] calculated the interfacial tension for an isotropic−nematic biphasic system assuming a stepwise conformation of molecules at the interface. McMullen[26] expressed the orientational distribution function in a series of spherical harmonics with the expansion coefficients represented by artificial hyperbolic profiles. Chen and Noolandi[27] superseded this theory by making no assumptions regarding the interfacial profile or orientation function and used numerical methods. They did not, however, consider the effects of the higher virial terms in the free energy density of the system. Koch and Harlen[29] used a generalization of the Onsager approach to determine the spatial orientational probability density that minimizes free energy, and recently the Doi and Kuzuu[25] theory has been extended by Chen and Sato[28] who used scaled particle theory and included third and fourth virial coefficients. One common result to all theories is that the surface tension is thermodynamically most stable (at the lowest surface tension value) when the rodlike molecules

(23) Katz, S.; Beatson, R. P.; Scallan, A. M. *Sven. Papperstidn.* **1984**, *87*, R48.
(24) Onsager, L. *Ann. N.Y. Acad. Sci.* **1949**, *51*, 627.
(25) Doi, M.; Kuzuu, K. *J. Appl. Polym. Sci.*: *Appl. Polym. Symp.* **1984**, *41*, 65.
(26) McMullen, W. E. *Phys. Rev. A.* **1988**, *38* (12), 6384.
(27) Chen, Z. Y.; Noolandi, J. *Phys. Rev. A* **1992**, *45* (4), 2389.
(28) Chen, W.; Sato, T. *Macromolecules* **1998**, *31*, 6506.
(29) Koch, D. L.; Harlen, O. G. *Macromolecules* **1999**, *32*, 219.

Table 2. pH, Debye Length, and Effective Cellulose Rod Diameter Data for Aqueous Suspensions of Microcrystalline Cellulose at 10 wt % Concentration

	acid added (mM)				
	0.1	0.5	1.0	1.5	3.0
pH	4.0	3.3	3.0	2.8	2.5
κ^{-1}/nm^{-1}	33.4	14.9	10.6	8.4	6.1
D_{eff}/nm	393	147	98	76	54

Table 3. Weight, Density, and Equivalent Cellulose Rod Diameter Data for Aqueous Suspensions of Microcrystalline Cellulose at 10 wt % Concentration

	acid (mM)				
	0.1	0.5	1.0	1.5	3.0
wt_{total}/g	0.103	0.094	0.112	0.108	0.098
wt_{iso}/g	0.088	0.071	0.109	0.105	0.097
wt_{aniso}/g	0.114	0.107	0.118	0.117	0.109
ρ_{iso}/g cm^{-3}	1.029	1.021	1.028	1.025	1.021
ρ_{aniso}/g cm^{-3}	1.038	1.032	1.046	1.034	1.036
$D_{eq\ iso}$/nm	23.2	19.0	18.7	19.5	21.2
$D_{eq\ aniso}$/nm	22.6	24.2	21.6	22.1	23.6
$D_{eq\ ave}$/nm	22.9	26.6	20.2	20.8	22.4

lie and align in the interfacial plane, that is, the nematic director lies at $\pi/2$ to the interface. When this condition is met, the equilibrium interfacial tension can be expressed in general terms:

$$\gamma = K\frac{k_B T}{DL} \tag{1}$$

where K is a constant depending on which theoretical approach has been adopted, for example, $K = 0.257$ (Doi and Kuzuu[25]), 0.34 (McMullen[26]), 0.18 (Chen and Noolandi[27]), and 0.316 (Koch and Harlen[29]); k_B is Boltzmann's constant; L and D are the contour length and diameter of the model, rigid spherocylinder.

As mentioned above, eq 1 holds if the nematic director is in the interfacial plane (i.e., the tilt angle is $\pi/2$). Optical and environmental scanning electron microscopy[12,22] experiments have shown that this criterion is met in the cellulose system, thus permitting calculation of $\gamma_{iso-aniso}$ from the rod dimensions. The values obtained from TEM experiments ($L = 180$ nm and $D = 8$ nm) could be used, but these are the hard core rod dimensions and the cellulose colloid suspensions are stabilized by electrostatic repulsion between the negatively charged sulfate ester groups. These soft electrostatic charges need to be incorporated into an effective diameter, D_{eff}, that is a function of both the geometric value, D, and the Debye radius, κ^{-1}, so D_{eff} is therefore sensitive to concentration and ionic strength. In the cellulose suspensions studied here, the only counterions present are hydrogen ions; hence κ^{-1} was determined using Manning's[30] approach and subsequently used to estimate D_{eff} from Onsager theory[12,24] for all concentrations and ionic strengths. Examples of such values for a 10 wt % suspension as a function of ionic strength are given in Table 2.

Chen and Gray[14] used a different approach to estimate rod diameter, again based on Onsager theory, but this time the experimental densities and weight fractions of the rods in each of the isotropic/anisotropic phases were involved in the calculation. This method was also applied here, and final values, given as D_{eq} in Table 3, were determined by taking the mean value from the coexisting phases. Details of calculations used in both methods are given in ref 14 (and references within). The values obtained for both rod diameters were subsequently substituted into eq 1 to estimate $\gamma_{aniso-iso}$ where $L = 180$ nm and the extremes of the constant value, $K = 0.18$ (Chen and Noolandi)[27] and $K = 0.34$ (McMullen),[26] were used. Comparing results given in Tables 2 and 3 reveals that D_{eff} values are considerably larger than D_{eq} and moreover D_{eff} increases rapidly with ionic strength in comparison to the static D_{eq} values. These differences are carried through the calculation and have influenced $\gamma_{aniso-iso}$. Furthermore, all calculated values for $\gamma_{aniso-iso}$ are approximately 2−3 orders of magnitude smaller in comparison to those obtained experimentally. In an attempt to understand the difference between experiment and theory, we re-examine the methods used to estimate the rod diameters, but it is difficult to predict which method of rod diameter calculation is more realistic. In the first method, the shortcomings of calculating the Debye length, and hence D_{eff}, at low ionic strength are evident at low quantities of added HCl as D_{eff} is unrealistically high, being twice the length of the rod. In the latter method, it was assumed that the interface was flat and that the bulk weight fractions and densities were representative of interfacial behavior. Nonuniformity of the interface would lead to interfacial roughness and hence an increase in $\gamma_{aniso-iso}$. Furthermore, treating the electrostatic repulsive forces as if they are uniformly distributed over each molecule is clearly an oversimplification but would influence both calculation methods. All shortcomings are carried through the interfacial tension calculation where we have made another assumption that Onsager theory holds for our system. Onsager's equations are only exact, however, under the conditions of high axial ratio and low rod concentration. Neither of these applied to the cellulose system studied here. Even the highest possible axial ratio value of 22 (using the hard core diameter) is outside the limit of high axial rod ratio, casting doubt over all predictions of $\gamma_{aniso-iso}$.

One interesting feature, however, is that the predicted $\gamma_{aniso-iso}$ values calculated using D_{eq} mimic the experimental trend as both show no significant dependency on ionic strength. The difference in magnitude between theory and experiment could be due to the sensitivity of our instrument as in this range small changes in contact angle could make a significant difference to the interfacial energy value. This is unlikely, however, as our instrument was calibrated carefully and results were highly reproducible. One explanation is possibly that true equilibrium values were not extracted from the images obtained, as the drop was not stable indefinitely. The polydispersity and presence of any aggregated flocs could also influence the experimental result but are not incorporated into any theoretical prediction. Presently, the only experimental technique that could be adopted to study equilibrium values is surface quasi-elastic light scattering.[31] This may prove difficult, however, due to the high number of molecules present in the isotropic phase causing multiple scattering events.

One final approach referred to by Chen and Gray[14] is the scaling theory of van der Schoot.[32] This method does not rely on the second virial coefficient approximation but instead relates interfacial tension to the osmotic pressure, p, and interfacial thickness, δ, via

$$\gamma = pf\delta \tag{2}$$

where f is a dimensionless scaling function that depends on the interfacial pressure gradient. $\gamma_{aniso-iso}$ values were

(30) Manning, G.; Zimm, B. H. *J. Chem. Phys.* **1965**, *43*, 4250.

(31) Buzza, D. M. A.; Jones, J. L.; McLeish, T. C. B.; Richards, R. W. *J. Chem. Phys.* **1998**, *22*, 5008.

(32) van der Schoot, P. *J. Phys. Chem.* **1999**, *103*, 8804.

Table 4. Experimental and Calculated Interfacial Tension Measurements for Cellulose Suspensions at 10 wt % Concentration

		acid (mM)				
		0.1	0.5	1.0	1.5	3.0
$\gamma_{aniso-iso\ expt}$/ mN m^{-1} × 10^{-2}		1.3	1.0	1.2	1.0	0. 8
$\gamma_{aniso-iso}$ using D_{eff}/ mN m^{-1} × 10^{-4}	$K = 0.18$[a]	0.1	0.3	0.4	0.6	
	$K = 0.34$[b]	0. 2	0.5	1.0	1.2	
$\gamma_{aniso-iso}$ using D_{eq}/ mN m^{-1} × 10^{-4}	$K = 0.18$[a]	1.7	1.6	2.1	2.0	1.9
	$K = 0.34$[b]	3.4	2.9	3.9	3.7	3.5
$\gamma_{aniso-iso}$ van der Schoot/ mN m^{-1} × 10^{-2}		0.33	0.34	0.43	0.40	0.35

[a] Chen and Noolandi. [b] McMullen.

therefore calculated using eq 2 and van der Schoot's approximation to estimate the interfacial width ($\delta = 1.33L = 240$ nm), the scaling factor $f \sim {}^1/_{10}$, and Lee's estimation of the osmotic pressure (~2.7).[19] The values calculated are given in Table 4 and are significantly closer to those obtained experimentally but are still $^1/_3$ lower. This is possibly due to the approximations made in parameter estimation; for example, the interfacial thickness value was purely a geometric estimate where δ_{iso} was estimated to be one rod length and δ_{aniso} was calculated using the tilt angle ($=\pi/2$) in conjunction with Onsager theory. We also assumed no critical demixing or accumulation of material occurred at the interface, and such conditions are unlikely to be met experimentally. Any of these deviations will cause the interfacial roughness to increase; hence $\gamma_{aniso-iso}$ will rise, bringing the value closer to experimental observations.

Further studies are under way to rigorously test theoretical predictions by investigating the influence of molecular weight and polydispersity (achieved by mixing known quantities of well-defined rods together) on surface and interfacial tension. It is hoped that this work will catalyze the extension of existing theories.

Conclusion

The surface tensions of the isotropic and anisotropic phases of rod suspensions of cellulose microcrystals have been determined as a function of suspension concentration and ionic strength. The results for individual ionic strengths gave similar trends as a function of concentration where cellulose rods in the isotropic regime were surface active as they reduced the surface tension of water by ~5 mN m^{-1} over all suspension concentrations. Contrasting such behavior, the cellulose rods that displayed liquid crystalline characteristics did not show any surface activity below c^{**} but became negatively surface active as the anisotropic concentration increased. As the ionic strength of each sample was increased, the surface tension of both phases increased, by ca. 2 mN m^{-1} over the range of concentrations investigated. All surface tension variation has been attributed to changes in the surface organization of the cellulose rods. The polar/nonpolar components have conformational freedom to find the lowest energy arrangement in the isotropic phase, while in the anisotropic media mobility is inhibited due to the intermolecular hydrogen bonding. The changes as a function of ionic strength were due to a decrease in Debye length as the screening of charges would decrease with increasing ionic strength, allowing the chains to move closer together and thus reducing their conformational freedom. Such changes are reflected in the higher surface tension values.

The interfacial surface tension between the coexisting phases has also been determined and is constant for all concentrations and ionic strengths. It is suggested that only the position of the interface is varied with concentration, and not the interfacial organization or concentration difference between each phase. The experimental values are higher than those predicted theoretically. We have demonstrated that scaling particle theory provides the closest prediction of experimental values, as other theories rely heavily on Onsager theory which is only valid in the limit of infinite axial ratio. The same qualitative trend was observed using the scaled particle theory, suggesting that the interfacial roughness was underestimated. One other explanation is the polydispersity of the cellulose rods, and this is currently undergoing investigation.

Acknowledgment. This work has been supported by EPSRC. Both authors thank Dr. I. Hopkinson for helpful discussions.

LA0258300